



## Reducing conservatism in highest density environmental contours

Andreas F. Haselsteiner<sup>a,\*</sup>, Ed Mackay<sup>b</sup>, Klaus-Dieter Thoben<sup>a</sup>

<sup>a</sup> University of Bremen, Institute for Integrated Product Development (BIK) and ForWind - Center for Wind Energy Research, Bremen, Germany

<sup>b</sup> University of Exeter, College of Engineering, Mathematics and Physical Sciences, Penryn, United Kingdom

### ARTICLE INFO

Dataset link: <https://github.com/ahaselsteiner/2020-paper-contour-conservatism>

#### Keywords:

Environmental contour  
Metocean extremes  
Design loads  
Reliability  
Marine structure

### ABSTRACT

Environmental contours are often used to define design loads acting on a marine structure. An environmental contour describes joint extremes of variables such as wave height, wave period and wind speed that are exceeded with a target return period. These extreme environmental conditions should lead to a structural response with a similar return period. Environmental contours can be defined based on different probabilistic definitions, one of them being that a contour surrounds a so-called highest density region. Highest density contours are a conservative concept that implies that any structure that is designed based on it will have an extreme response that has a return period that is higher than the contour's return period (when short-term variability is accounted for). For some structures, however, the design loads are overly conservative because in the contour construction phase also environmental conditions, which will clearly not lead to an extreme response, are counted as exceedance. Here, we show how this over-conservatism can be avoided by predefining a region in the variable space that will not lead to extreme loads. We give an example, where we define such "mild regions" for sea state contours. By assuming a structural response, we explore the effect of mild regions on the estimated extreme response. In the presented example, a normal highest density contour leads to a design response that is 13% too conservative, while a contour that is adjusted using a reasonable mild region can reduce conservatism to 7%.

### 1. Introduction

When the reliability of a marine structure is investigated, often the so-called environmental contour method is utilized. It is widely used in practice, which can be inferred by its presence in authoritative guidelines (DNV GL, 2017) and standards (International Electrotechnical Commission, 2019). The method has been used to analyze wind turbines (Saranyasontorn and Manuel, 2006a,b; Myers et al., 2015; Karmakar et al., 2016; Liu et al., 2019; Velarde et al., 2019; Chen et al., 2020; Haselsteiner et al., 2021), wave energy converters (Muliawan et al., 2013; Coe et al., 2018; Neary et al., 2020), an integrated wind-wave-tidal energy converter (Li et al., 2019), floating structures for oil and gas production (Winterstein et al., 1999; Silva-González et al., 2015; Wang et al., 2018), bridges (Xu et al., 2018; Giske et al., 2018) and vessels (Armstrong et al., 2015; de Hauteclocque et al., 2021). To analyze the long-term response of a structure, the method provides an efficient approximation to a full long-term analysis (FLTA). An environmental contour consists of joint extremes of environmental conditions such as wave height, wave period and wind speed that will be used to define design loads that act on the structure of interest. The joint extremes are derived based on a prescribed target return period, for example,  $N = 50$  years, and the idea is that these joint environmental

extremes cause an extreme response with a return period of circa  $N$  years as well. To ensure the reliability target, this estimated extreme response's return period is not allowed to be less than  $N$  years, but to avoid over-conservatism it should not be much higher than  $N$  years too.

Environmental contours are solely derived from the joint distribution of metocean variables. Because different types of marine structures can have strongly different response characteristics, there is no fixed relationship between environment and response. Therefore, to ensure that a  $N$ -year environmental extreme does not lead to a response with a return period of less than  $N$  years, some conservatism is required in the definition of what constitutes an  $N$ -year environmental extreme and therefore an  $N$ -year environmental contour. As multivariate statistics does not provide a unique definition for multivariate quantiles (see, for example, Einmahl et al., 2013; Serinaldi, 2015), defining an  $N$ -year extreme means defining the characteristics of a quantile region, or its complementary, the characteristics of an exceedance region. Since the first papers on the method (Haver, 1985, 1987; Winterstein et al., 1993), researchers have proposed different contour methods based on different concepts of exceedance. These methods include methods that are direct analogs of univariate extremes, defined as the

\* Corresponding author.

E-mail addresses: [a.haselsteiner@uni-bremen.de](mailto:a.haselsteiner@uni-bremen.de) (A.F. Haselsteiner), [e.mackay@exeter.ac.uk](mailto:e.mackay@exeter.ac.uk) (E. Mackay).

intersection of multiple univariate exceedance regions under rotations of the coordinate system (Winterstein et al., 1993; Huseby et al., 2013; Derbanne and de Hauteclocque, 2019), joint exceedance regions that are bounded by one threshold value per variable (Jonathan et al., 2014), exceedance regions that fully enclose the contour (Haselsteiner et al., 2017; Chai and Leira, 2018; Dimitrov, 2020) and exceedance regions that are designed for specific variable combinations, such as wave height and wave period (Haver, 1985, 1987). A review on the variety of contour methods is provided in Ross et al. (2019) and the results of a benchmarking exercise on contour methods is presented in Haselsteiner et al. (2021a). Mackay and Haselsteiner (2021) analyzed four contour methods and discussed the implications the different definitions of exceedance have on the design process. For a given joint distribution and a given contour exceedance probability,  $\alpha$ , these contour methods lead to different environmental design conditions and therefore to different load assumptions.

Probably the most widely used contour method is based on the framework of the inverse first-order reliability method (IFORM). The original method was proposed by Winterstein et al. (1993) who constructed contours in standard normal space, which are exceeded with probability  $\alpha$  in each direction  $\theta \in [0, 360)$ . Huseby et al. (2013) proposed to use a similar definition of exceedance, however, in the original variable space. These definitions of marginal exceedance under rotations of the variable space are supported by the idea that, when the structure is designed to have a capacity that withstands the highest load along this contour, the failure boundary can often be conservatively approximated as a straight line that touches the contour at the point of highest response (called the “design point” in the IFORM framework). This approximation is appropriate for many marine structures, especially in the significant wave height–wave period variable space (see, for example, Armstrong et al., 2015; de Hauteclocque et al., 2021). For some structures and some environmental variable combinations, however, the IFORM contour definition (Winterstein et al., 1993) and its equivalent in the original variable space (Huseby et al., 2013; Derbanne and de Hauteclocque, 2019) can underestimate the size of the failure region. In these cases, if design loads are derived from an IFORM contour and the structure is designed to withstand only these loads, the true probability of failure will be higher than the target probability of failure (Mackay and Haselsteiner, 2021). This problem occurs if the failure region is concave at the point that touches the environmental contour. This can happen, for example,

- for contours in the significant wave height–wave period variable space if the structure has two distinct eigenfrequencies (Mackay and Haselsteiner, 2021);
- for contours in the wind speed–wave height variable space if offshore wind turbines are analyzed (Saranyasontorn and Manuel, 2006b; Li et al., 2016, 2017; Haselsteiner et al., 2021); and
- for directional environmental contours where contours are defined for the  $x$  and  $y$  component of wind speed (Vanem et al., 2019) or significant wave height (Haghighyehi and Ketabdari, 2018; Mackay and Haselsteiner, 2021).

Fig. 1 shows three such examples. Another way how IFORM’s approximation of the failure region can become non-conservative is if a single structure has multiple response variables that have their highest response at different regions of the contour. This is for example the case in offshore wind turbine design (Haselsteiner et al., 2021). Consider the bending moment of a turbine’s support structure, a monopile, at various water depths. The center of pressure of wave forces is at a much lower height than the center of pressure of wind forces. Consequently, the relative contribution of wave forces on the overall bending moment increases as the water depth increases. Thus, highest value along the contour of the 5 m moment occurs ca. at  $15 \text{ m s}^{-1}$  wind speed, but for the 30 m moment it occurs at ca.  $35 \text{ m s}^{-1}$  wind speed (Fig. 2). If the monopile’s wall thickness is optimized based on the highest bending moment values along the contour at both heights, two individual failure

regions will touch the contour at two distinct wind speed values. The monopile’s overall failure region is the union of the individual failure regions of the two (or more) response variables. Thus, the overall failure region is non-convex and contains a probability greater than  $\alpha$ .

To avoid to design an unreliable structure in these cases, an environmental contour that is defined based on “total exceedance probability” can be used (Haselsteiner et al., 2017; Chai and Leira, 2018; Dimitrov, 2020; Mackay and Haselsteiner, 2021). Such contours are defined such that the probability that a contour is exceeded anywhere is  $\alpha$ . The definition of total exceedance probability can also be interpreted as approximating the failure region to fully surround the contour. Thus, this contour definition will always yield conservative design loads. Total exceedance contours include the highest density contour (Haselsteiner et al., 2017), which is defined in the original variable space, and Chai and Leira’s ISORM contour (Chai and Leira, 2018), which is defined in standard normal space.

In this work, we will focus on the highest density (HD) environmental contour method (Haselsteiner et al., 2017) and for simplicity, we will assume that the marine structure has a deterministic response and that short-term (for example, hourly) environmental conditions are independent and identically distributed. Using an exceedance region that fully surrounds the contour is the most conservative assumption one can make when defining an environmental contour: A structure’s failure probability,  $p_f$ , is equal the exceedance region’s probability content,  $\alpha$ , only if the failure region fully surrounds the contour as well. In all other shapes of the failure region, the structure’s failure’s probability is less than  $\alpha$ . While this definition avoids the possibility of designing an unreliable structure, it leads to some over-conservatism. Here, we will show how regions, of which the analyst is certain that they will not cause failure-relevant loads, can be excluded from the set that defines the exceedance region. That way over-conservatism can be avoided.

The paper is organized as follows. Section 2 describes how a highest density contour can be modified to contain only severe conditions. An example of the effect of excluding mild conditions for a sea state contour is presented in Section 3. Finally, a discussion and conclusions are presented in Sections 4 and 5.

## 2. Defining the exceedance region to contain only severe conditions

A highest density environmental contour is defined in Haselsteiner et al. (2017) to be the boundary of a highest density region,  $R_{HD}$ , which can be expressed as the set of all environmental conditions  $\mathbf{x}$  whose probability density is greater than a threshold  $f_m$ :

$$R_{HD}(f_m) = \{\mathbf{x} \in \mathbb{R}^d : f(\mathbf{x}) \geq f_m\}, \quad (1)$$

where  $f(\mathbf{x})$  is the joint density function and  $f_m$  is chosen as the largest threshold that yields a region, which contains a probability of at least  $1 - \alpha$ , that is

$$f_m = \underset{f \in (0, \infty)}{\operatorname{argmax}} \Pr(\mathbf{X} \in R_{HD}(f)) \geq 1 - \alpha. \quad (2)$$

Then, the  $\alpha$ -exceedance highest density contour is defined as the set  $C \subset R_{HD}$  that contains exactly the environmental states at which the probability density equals  $f_m$ .

Sometimes, however, it is clear that a certain region in the variable space will not lead to high loads and consequently will not be part of the failure region of the response of any structure that is designed based on an environmental contour. Here, we show how environmental conditions of this region can be excluded from being counted as exceedance. Let  $R_M$  denote this “mild region” that contains non-severe or “mild” environmental conditions. For example, consider a sea state contour, which describes joint extremes of significant wave height  $H_s$  and, say, zero-up-crossing period  $T_z$ . In such a contour, the region in the variable space below the contour’s lower  $H_s$  boundary, will not

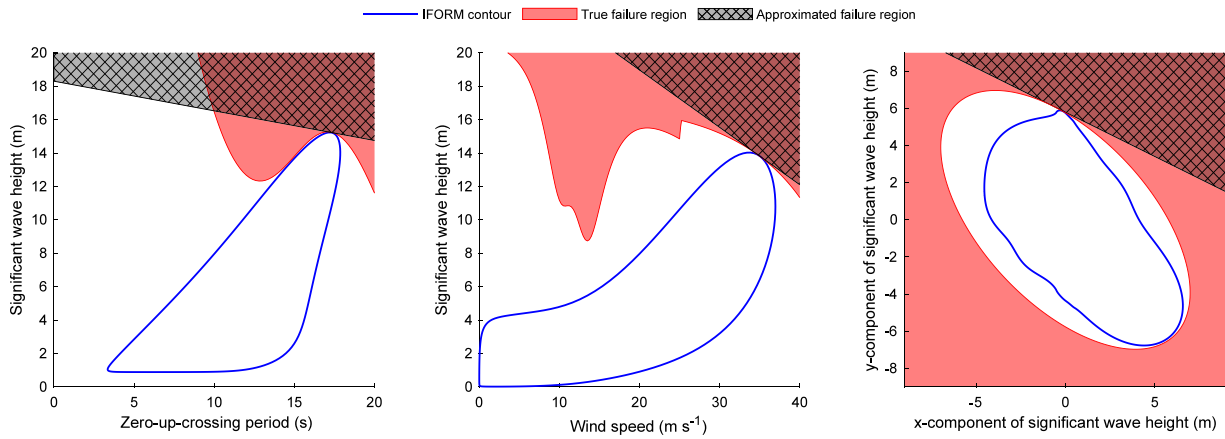


Fig. 1. Examples of single responses where the approximation of the failure region of an IFORM (Winterstein et al., 1993) or direct sampling (Huseby et al., 2013) environmental contour is non-conservative. In these cases a highest density contour can be used to provide conservative design loads. Left: A response with two distinct eigenfrequencies (Mackay and Haselsteiner, 2021). Middle: The 10 m bending moment of an offshore wind turbine (Haselsteiner et al., 2021). Right: A response of a structure that is designed to be stronger in the direction of the highest waves (Mackay and Haselsteiner, 2021).

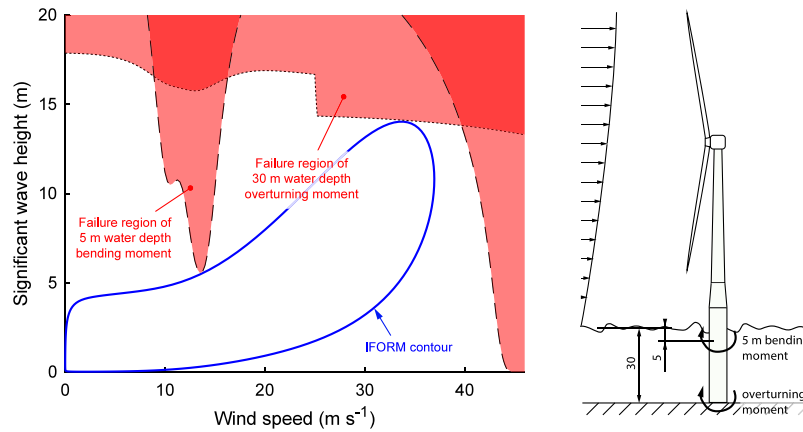


Fig. 2. Example how the combination of multiple response variables can cause the IFORM approximation to become non-conservative. Shown are failure surfaces from response variables relevant to the design of offshore wind turbine foundations. The relative contribution of wave forces is greater for the moment at 30 m than for the moment at 5 m water depth (Haselsteiner et al., 2021). Consequently, their failure regions have different shapes and touch the contour at different positions. The overall failure region is the union of the two individual failure regions. It contains more than  $\alpha$  probability.

be part of the failure region of any conceivable structure (Fig. 3). If one is certain that the environmental conditions in this region will not cause failure-relevant loads, the region should not be counted as exceedance. Instead it should be part of the design region, the region of the environmental variable space that the structure is designed to safely withstand. The design region is the complement of the exceedance region, containing  $1 - \alpha$  probability. Then, because the probability content is added to the design region, the design region must contract at other areas to not exceed  $1 - \alpha$  probability. In the  $H_s - T_z$  contour example, the contour would contract at the region of higher  $H_s$  values such that its environmental design conditions would lead to lower loads.

Another way to describe the concept is to consider that a designer wants to define a set of environmental conditions – a design region –, which fulfills two criteria:

1. It contains  $1 - \alpha$  probability such that the structure of interest has a probability of failure that is less than  $\alpha$  if the structure survives all loads that arise from these environmental conditions.
2. The region contains the area in the variable space of which the designer is certain that it is not problematic. Additionally, it contains as little area in the variable space as possible.

Adding a highest density region to the mild region such that they together form a design region with  $1 - \alpha$  probability content fulfills

these criteria. The mild region is based on engineering judgment that depends on the particular variable space and the particular structure under consideration. However, as  $\alpha$  is typically very low, additional area must be added to the design region to reach  $1 - \alpha$  probability. A highest density region requires the smallest possible space for a given probability content (Hyndman, 1996) such that its definition is advantageous in the area that holds possibly severe environmental conditions. In the following the concept of adjusting a highest density contour by considering a “mild region” is formally described.

### 2.1. Analytical definition

To avoid having non-severe conditions in the  $\alpha$ -exceedance region, we define the design region,  $R_D$ , as the union of a highest density region,  $R_{HD}$ , and a predefined mild region,  $R_M$ :

$$R_D = R_{HD} \cup R_M. \tag{3}$$

The complement of the design region, the  $\alpha$ -exceedance region, does not contain the mild region’s non-severe environmental conditions. To construct such a design region, first the mild region,  $R_M$ , is defined based on case-specific engineering judgment, which the analyst uses to define ranges of variables. Then, a highest density region must be found, which – in union with the mild region – contains  $1 - \alpha$

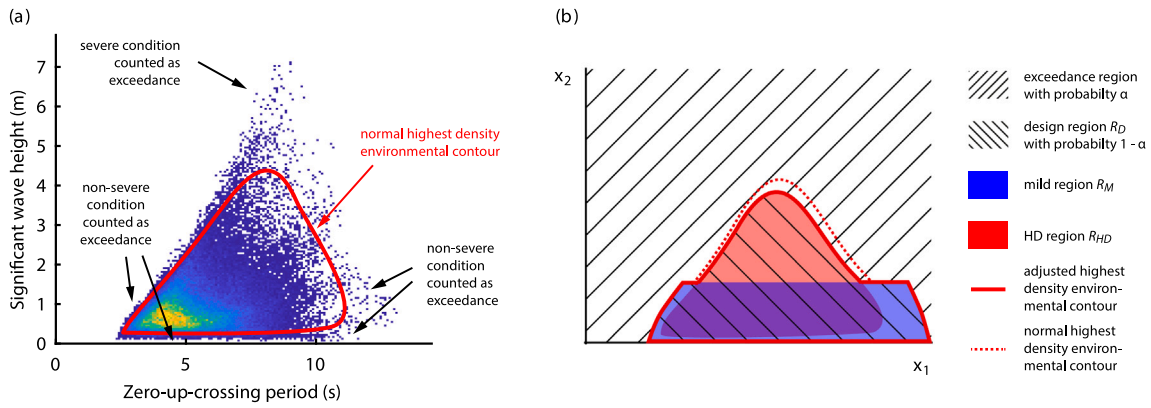


**Fig. 3.** Motivation for adjusting a highest density contour. (a) In some variable spaces it is clear that the environmental conditions in certain regions will not cause structural failure because they hold non-severe or “mild” environmental conditions. When these regions are part of the exceedance region that holds a probability of  $\alpha$ , a normal highest density contour will be overly conservative. (b) Non-severe conditions can be excluded from the exceedance region by defining a “mild region”. Then the exceedance region must spread to additional regions in the variable space to hold a probability of  $\alpha$ .

probability:

$$f_a = \operatorname{argmax}_{f \in [0, \infty)} \Pr(\mathbf{X} \in R_{HD}(f) \cup R_M) \geq 1 - \alpha. \quad (4)$$

As defined in (3) the design region is then found by calculating the union of the highest density region,  $R_{HD}$ , and the mild region,  $R_M$ . The adjusted highest density environmental contour is the boundary of the design region. Note that for the same exceedance probability  $\alpha$ , the density value  $f_a$  of the adjusted contour will be higher than the density value of a normal highest density contour  $f_m$  (compare Eqs. (2) and (4)).

Based on this definition, the variable space is divided into two regions: A design region that holds  $1 - \alpha$  probability and an exceedance region that holds  $\alpha$  probability. The definition will result in a contour that is smaller in the non-mild region than a pure highest density contour such that its design conditions will be less conservative. However, as long as a structure’s failure region is contained in the exceedance region,  $N$ -year design conditions will lead to a conservative estimation of the  $N$ -year response (assuming a deterministic response).

The case-specific conservatism of an environmental contour can be evaluated by variables that relate response characteristics associated with the contour to ideal response characteristics. We define the conservatism number  $\gamma_r$  to relate the strongest response along the contour,  $\hat{r}_N$  to the true  $N$ -year response  $r_N$ :

$$\gamma_r = \frac{\hat{r}_N}{r_N}. \quad (5)$$

Further, we define the conservatism number  $\gamma_{pf}$  to relate the failure probability that a structure has that fails if  $\hat{r}_N$  is exceeded to the target failure probability  $\alpha$ :

$$\gamma_{pf} = \frac{\alpha}{1 - F_R(\hat{r}_N)} = \frac{\alpha}{p_f}, \quad (6)$$

where  $F_R$  is the long-term response function, which can be estimated using a full long-term analysis (see, for example, Sagrilo et al., 2011; Muliawan et al., 2013; Vanem et al., 2020; Haselsteiner et al., 2021).

If the conservatism numbers  $\gamma_r$  and  $\gamma_{pf}$  are less than 1, the contour describes non-conservative design conditions and if they are greater than 1 the contour describes conservative design conditions. The goal is to construct a contour that will result in  $\gamma_r \geq 1$ , but close to 1 and in  $\gamma_{pf} \geq 1$ , but close to 1. Note that calculating these conservatism numbers requires a full long-term analysis such that they are useful in characterizing contour methods as we do in this study, but not in practical applications where no FLTA is performed.

### 2.2. Numerical implementation

The contours were constructed using a numerical integration scheme that is similar to the scheme described in Haselsteiner et al. (2017). First, a region in the variable space that contains almost the complete probability content is separated into  $n$  cells, where each cell has a unique index  $i \in [1, n]$ .

The probability contained in cell  $i$ ,  $p_i$ , is approximated by multiplying the marginal probabilities contained within this cell:

$$p_i = [F_x(x_i^u) - F_x(x_i^l)] \times [F_{y|x}(y_i^u|x_i^c) - F_{y|x}(y_i^l|x_i^c)], \quad (7)$$

where  $x_i^l$ ,  $x_i^c$ ,  $x_i^u$  represent the  $x$  coordinates of the cell’s lower boundary, center and upper boundary, respectively, and  $y_i^l$  and  $y_i^u$  upper and lower boundary of the  $y$  coordinate.  $F_x$  represents the marginal distribution function of  $X$  and  $F_{y|x}$  represents the conditional cumulative distribution function of  $Y$  given  $X$ .

Based on this probability, the average probability density for each cell is calculated by dividing by the cell size:

$$\bar{f}_i = \frac{p_i}{\Delta x \Delta y}. \quad (8)$$

After having calculated  $p_i$  and  $\bar{f}_i$  for all cells with indices  $i = \{1, \dots, n\}$ , Eq. (4) is numerically solved by first defining a function that returns the probability contained in  $R_{HD}(f) \cup R_M$ ,

$$G(f) = \Pr(\mathbf{X} \in R_{HD}(f) \cup R_M) \approx \sum_i p_i : \bar{f}_i \geq f \vee \begin{pmatrix} x_i \\ y_i \end{pmatrix} \in R_M, \quad (9)$$

and then solving the root finding problem,

$$G(f) - 1 + \alpha = 0, \quad (10)$$

which returns the density value  $f_a$  that approximates Eq. (4). This scheme is sensitive to the used grid resolution and position and it is necessary to check the cell size is small enough to ensure grid independence. In the following example, the grid cells had a size of  $0.05 \text{ m} \times 0.05 \text{ s}$  (wave height  $\times$  wave period).

### 3. Example: Environmental contour for sea states

Possibly the most common use case of environmental contours is constructing such a contour for sea states that are described with the variables significant wave height,  $H_s$ , and a variable that describes the sea states frequencies, for example, zero-up-crossing period,  $T_z$ . In this example, we use a model for the joint distribution of  $H_s$  and  $T_z$  that has been used in many previous studies on environmental contours (see, for example, Vanem and Bitner-Gregersen, 2012; Haselsteiner et al., 2017; Huseby et al., 2013; Chai and Leira, 2018; Mackay and Haselsteiner,

2021). The model describes sea states with a duration of  $T_S = 6$  hours and assumes that significant wave height follows a translated Weibull distribution:

$$F_{H_s}(h_s) = 1 - e^{-[(x-\gamma)/\alpha]^\beta}, \quad (11)$$

where  $\alpha = 2.776$ ,  $\beta = 1.471$  and  $\gamma = 0.8888$ .

Zero-up-crossing period follows a conditional log-normal distribution:

$$F_{T_z|H_s}(t_z|h_s) = \frac{1}{2} + \frac{1}{2} \operatorname{erf} \left[ \frac{\ln t_z - \mu}{\sqrt{2}\sigma} \right], \quad (12)$$

where  $\mu = 0.1 + 1.489h_s^{0.1901}$  and  $\sigma = 0.04 + 0.1748 \exp(-0.2243h_s)$ .

Consider that a marine structure has been designed that responds with a deterministic response function that responds strongly at two distinct frequencies, which could be the effect of the two eigenperiods  $t_{e1}$  and  $t_{e2}$ :

$$r(h_s, t_p) = a_1 \frac{h_s}{1 + b_1(t_p - t_{e1})^2} + a_2 \frac{h_s}{1 + b_2(t_p - t_{e2})^2}, \quad (13)$$

where  $a_1 = 4$ ,  $a_2 = 1.1$ ,  $b_1 = 0.1$ ,  $b_2 = 0.05$ ,  $t_{e1} = 25$  s,  $t_{e2} = 12.5$  s and  $t_p = 1.2796t_z$  (Mackay and Haselsteiner, 2021). This function is the sum of two response functions of the form given in Ross et al. (2019) and serves to describe a case where the IFORM approximation is non-conservative such that a highest density contour might be considered. The response function has been considered in a previous study (Mackay and Haselsteiner, 2021) and – as expected – it was found that when the 50 year response is estimated, IFORM and direct sampling contours can lead to non-conservative response estimates, while ISORM and highest density contours lead to overly conservative response estimates.

Here, we found that the highest response along a normal highest density contour is 19.2<sup>1</sup> while a full long-term analysis lead to a response of 17.0. Thus the estimated response is 13% too high ( $\gamma_r = 1.13$ ). If the structure is designed to have a capacity of exactly the estimated 50 year response, the probability of failure would be about six times the target probability of failure ( $\gamma_{pf} = 5.8$ ). These results show that in this case, the normal highest density contour leads to significant over-conservatism, which could be reduced by defining a mild region and adjusting the contour.

To test the influence of the mild region, we tested eight different mild regions that vary in their size. We considered environmental conditions to be mild, which have a significant wave height smaller than {2, 4, 6, 8, 10, 12, 14, 15.23} m, where, in this example, the marginal 50 year  $H_s$  return value is 15.23 m. To avoid extending the mild region into areas of the parameter space which do not occur, we also require that all points in the mild region have a non-zero probability density (Fig. 4). In the present example, however, environmental conditions with a probability density greater than  $10^{-9}$  rather than zero were used, since the log-normal distribution used for the value of  $T_z$  conditional on  $H_s$  is only exactly zero for  $T_z = 0$  or  $\infty$ . This is a problem of the considered distribution function. Nevertheless, we use this distribution as it allows direct comparison to other academic studies (Vanem and Bitner-Gregersen, 2012; Haselsteiner et al., 2017; Huseby et al., 2013; Chai and Leira, 2018; Mackay and Haselsteiner, 2021), which used it too. The threshold for the probability density was selected by choosing a value that is multiple orders of magnitude lower than the density value of a normal 50 year highest density contour. Its purpose is to provide a boundary in the  $T_z$  direction as otherwise also nonphysical values, for example, hindered by wave breaking, would be included in the design region.

Fig. 5 shows one of the considered mild regions, together with the corresponding adjusted 50 year contour, the unadjusted 50 year contour and some lines of constant response. The shown mild region

reaches up to  $H_s = 8$  m, which is about 50% of the marginal 50 year  $H_s$  return value ( $H_{s,50} = 15.23$  m). The maximum  $H_s$  value along the adjusted HD contour is 16.43 m, while the maximum  $H_s$  value along the unadjusted HD contour is 16.81 m. The adjusted contour's response estimate is about 9% higher than the “true” response and the probability of failure is about three times lower than the target probability of failure. Among the tested mild regions, the 50 year response estimator decreases as the mild region's  $H_s$  threshold increases (Table 1). Consequently, the conservatism numbers  $\gamma_r$  and  $\gamma_{pf}$  decrease. However, at a  $H_s$  threshold of 14 m, the response increases because the highest response along the contour occurs at a segment belonging to the mild region instead of the highest density region (Fig. 6).

Overall, among the considered mild regions that reduced conservatism, the estimated responses were between 5% and 12% too high, while the unadjusted HD contour lead to a response, which is 13% too high. In practice, designers would not make a parameter study as here, but choose one mild region without knowing the structure's true response. In this example, a reasonable choice for the mild region's  $H_s$  threshold could be between 30% and 70% of the marginal  $H_{s,50}$  value suggesting a threshold between 4.6 and 10.6 m. In the outline example, choosing such a mild region would have reduced the conservatism number to  $\gamma_r = 1.07$  to 1.11 meaning the design response would be 7%–11% too high.

## 4. Discussion

### 4.1. Mild significant wave height

In the presented example one variable was significant wave height. Because the response of most marine structure increases with  $H_s$ , we used mild regions that cover low  $H_s$  values for a given wave period. The assumption that the structural response increases with  $H_s$  could also be used to include all environmental conditions that are below a contour's upper  $H_s$  boundary into the mild region. For the sea state example, that would mean that even sea states with, say,  $H_s = 12$  m are considered mild at  $T_z = 13$  s because the environmental contour holds sea states with  $H_s > 15$  m at  $T_z = 13$  s (Fig. 5). This would add some additional environmental states to the design region such that its dimensions would decrease at other areas.

However, such a definition for the mild region would be based on the contour's coordinates. Thus, the mild region's dimensions could not be predefined, but would be calculated in conjunction with the contour. Here, we aimed to introduce the concept of using a mild region using a simple example such that we did not pursue the joint calculation of mild region and contour. However, adding all conditions where  $H_s$  is smaller than the contour's  $H_s$  could be used to reduce some additional unnecessary conservatism.

Interestingly, if a mild region were used that is solely based on the condition that all  $H_s$  are mild that are below a contour's upper  $H_s$  boundary, the resulting contour would be relatively similar to a contour based on the method Haver presented in 1985 (Haver, 1985). Haver proposed to define a sea state “design curve”  $h_{s,curve}(t_z)$  by setting two conditions: (1) overall exceedance of the curve is  $\alpha$ ; and (2) along the curve the conditional exceedance,  $\Pr(H_s \leq h_{s,curve}(t_z) | T_z = t_z)$ , is constant.<sup>2</sup> In contrast to a highest density contour, Haver's contour does not have constant probability density along its curve, however, due to the overall exceedance probability of  $\alpha$  and the similarity of the regions where sea states are counted as exceedances, the curves would likely be similar.

<sup>2</sup> Here, we used zero-up-crossing period  $T_z$ , while Haver (1985) used spectral peak period  $T_p$ . Additionally, Haver restricted the “design curve” to span a predefined  $T_p$  interval.

<sup>1</sup> In Mackay and Haselsteiner (2021) we reported a slightly different response of 19.1, which is due to a different numerical implementation.

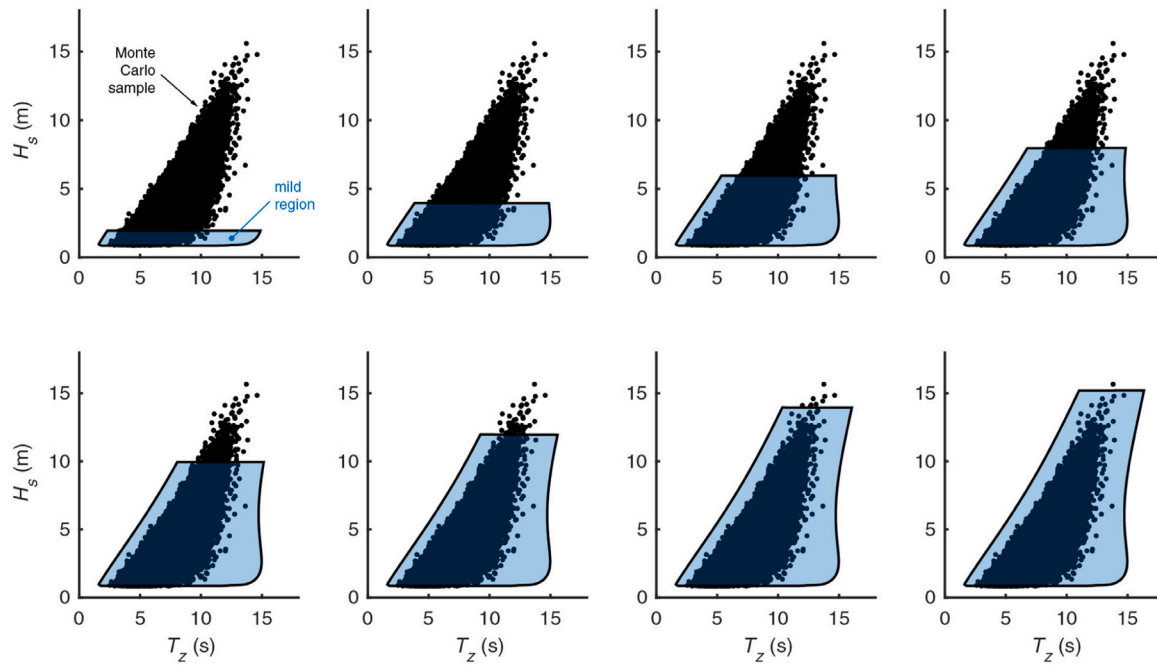


Fig. 4. Considered mild regions (shaded areas) and a Monte Carlo sample of sea states ( $n = 100,000$ ). Sea states that had a significant wave height smaller than  $\{2, 4, 6, 8, 10, 12, 14, 15.23\}$  m were considered mild.

Table 1

Responses based on environmental contours with different mild regions. Mild regions contain environmental conditions up to a threshold value of  $H_{s,m}$ . For reference, results for IFORM contours and for the full long-term analysis (FLTA) are reported too. We consider the result from the FLTA to be the true 50-year response that served as a reference value in this study. The exceedance probability is  $\alpha \approx 1.37 \times 10^{-5}$ .

| Method                    | $H_{s,m}$ (m) | Max. $H_s$ (m)                        | 50-year response $\hat{r}_{50}$                 | $\gamma_r = \frac{\hat{r}_{50}}{r_{50}}$ | $\gamma_{pf} = \frac{\alpha}{p_f}$   |
|---------------------------|---------------|---------------------------------------|---|--|--------------------------------------|
| Normal HD contour         | 0             | 16.81                                 | 19.2  | 1.13                                     | 5.8                                  |
| Adjusted HD contour       | 2             | 16.76                                 | 19.1  | 1.12                                     | 5.4                                  |
| Adjusted HD contour       | 4             | 16.65                                 | 18.9  | 1.11                                     | 4.7                                  |
| Adjusted HD contour       | 6             | 16.54                                 | 18.7  | 1.10                                     | 4.1                                  |
| Adjusted HD contour       | 8             | 16.43                                 | 18.4  | 1.09                                     | 3.4                                  |
| Adjusted HD contour       | 10            | 16.30                                 | 18.2  | 1.07                                     | 3.0                                  |
| Adjusted HD contour       | 12            | 16.13                                 | 17.9  | 1.05                                     | 2.3                                  |
| Adjusted HD contour       | 14            | 15.86                                 | 22.3  | 1.31                                     | 26.6                                 |
| Adjusted HD contour       | 15.23         | 15.35                                 | 26.5  | 1.56                                     | 112.6                                |
| IFORM contour             | –             | 15.23 (Mackay and Haselsteiner, 2021) | 16.57 (Mackay and Haselsteiner, 2021)           | 0.97 (Mackay and Haselsteiner, 2021)     | 0.61 (Mackay and Haselsteiner, 2021) |
| FLTA, “true” return value | –             | –                                     | $r_{50} = 17.0$ (Mackay and Haselsteiner, 2021) | 1  | 1                                    |

#### 4.2. When should mild regions be used?

In our opinion, the presented approach of using “mild regions” adds another option to the ways environmental contours can be constructed. In applications such as offshore wind turbine design where the environmental contour method is a recommended approach to estimate the  $N$ -year extreme response (International Electrotechnical Commission, 2019), designers need to decide which type of contour they construct. A decision tree which could be used to select one of the many contour methods is shown in Fig. 7. First, one considers whether the failure surface can be reasonable approximated linearly — this is the case if the failure region is convex. If the failure region is convex, a contour method that assumes a linear failure surface should be used, such as IFORM (Winterstein et al., 1993), the direct sampling method (Huseby et al., 2013, 2015) or direct IFORM (Derbanne and de Hauteclocque, 2019). If the failure region is not convex, the previously mentioned contour methods can lead to an extreme response with a lower return period than the contour’s return period. This means that one can end up with too low design loads. Thus, for non-convex failure regions, a contour that is defined based on total exceedance probability should be used. This class of contours includes Haver’s design curve

method (Haver, 1985), the highest density method (Haselsteiner et al., 2017), Chai and Leira’s ISORM (Chai and Leira, 2018) and Dimitrov’s inverse directional simulation method (Dimitrov, 2020). In case the highest density method is used and the bias due to ignoring the response’s short-term variability is controlled for, the resulting design loads will be too high (the  $N$ -year contour will cause a response with a return period higher than  $N$  years (Mackay and Haselsteiner, 2021)). If such overly conservative design loads are of concern in the application of interest, a mild region can be defined to reduce the contour’s dimensions at high environmental conditions such that the resulting design loads become lower.

#### 5. Conclusions

This work presented an approach to reduce the conservatism associated to highest density environmental contours that is based on redefining a so-called mild region. The mild region is defined on an engineer’s judgment of where in the variable space the structure will with certainty not experience failure due to extreme loads. The union of this mild region and the highest density region must contain  $1 - \alpha$  probability. Because the mild region holds some probability that would

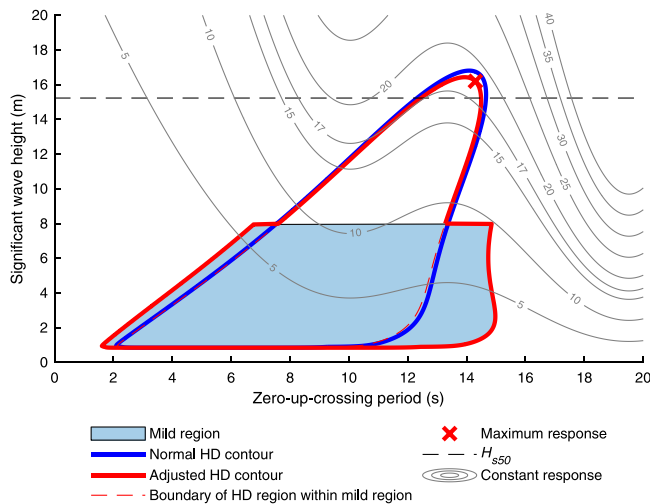


Fig. 5. Normal and adjusted 50 year highest density contour. Sea states with an intensity of less than 8 m significant wave height were included into the mild region.

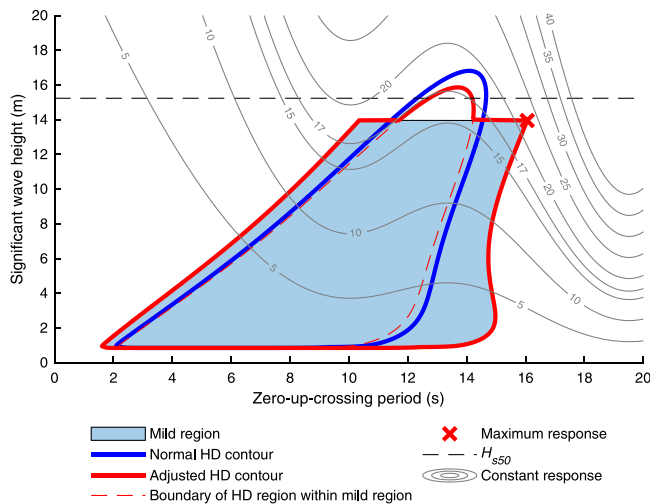


Fig. 6. 50 year sea state contour with an oversized mild region. The maximum response occurs at the mild region's boundary such that the mild region does not decrease conservatism.

not be contained in a normal highest density contour, the adjusted contour shrinks at the regions outside the mild region, which reduces the design loads that are associated with the conditions along the contour.

An application example of such adjusted environmental contours was presented: A sea state contour with a deterministic response function that could represent a marine structure with two distinct eigen-frequencies. We found that the adjusted environmental contours only shrink slightly if reasonable mild regions are used. The overestimation of the response was reduced from 13% to 7% if wave heights below 10m were considered mild. The effect on the failure probability was stronger though: While the normal highest density contour had a failure probability that was about six times smaller than the target failure probability the aforementioned adjusted contour had a failure probability that was about three times smaller than the target failure probability.

The example showed that mild regions can be defined based on general engineering judgment and using these mild regions reduces the dimensions of the environmental contours. However, the influence on the environmental design conditions and consequently on the loads and responses was found to be rather smaller, suggesting that other steps

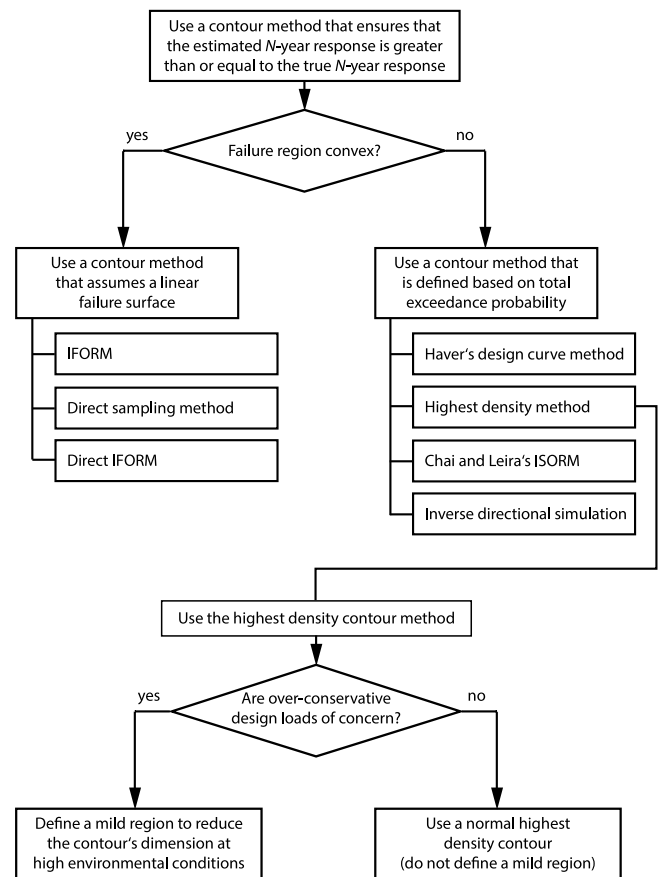


Fig. 7. Flow chart describing in which cases the use of a highest density contour method is appropriate and when to use a mild region. The various contour methods are described in the papers by Winterstein et al. (1993) (IFORM), Huseby et al. (2013) (direct sampling method), Derbanne and de Hauteclocque (2019) (direct IFORM), Haver (1985) (design curve method), Haselsteiner et al. (2017) (highest density method), Chai and Leira (2018) (ISORM) and Dimitrov (2020) (inverse directional simulation).

in the environmental contour method such as choosing an appropriate model for the joint distribution or deciding between using an contour method based on total exceedance or marginal exceedance likely have a bigger influence on the assumed design loads. The outlined approach of using a mild region adds to the options how environmental contours can be constructed. It is likely to be most useful for applications where the failure region is non-convex and it is important that design loads are not overly conservative.

**CRedit authorship contribution statement**

**Andreas F. Haselsteiner:** Conceptualization, Methodology, Software, Formal analysis, Writing – original draft, Writing – review & editing, Visualization. **Ed Mackay:** Conceptualization, Methodology, Writing – review & editing. **Klaus-Dieter Thoben:** Supervision.

**Declaration of competing interest**

The authors declare that they have no known competing financial interests or personal relationships that could have appeared to influence the work reported in this paper.

**Data and code availability**

The analysis of the example presented in Section 3 can be reproduced by running the MATLAB file Example1.m that is available at the GitHub repository <https://github.com/ahaselsteiner/2020-paper-contour-conservatism>.

## References

- Armstrong, C., Chin, C., Penesis, I., Drobyshevski, Y., 2015. Sensitivity of vessel responses to environmental contours of extreme sea states. In: Proc. 34th International Conference on Ocean, Offshore and Arctic Engineering, OMAE 2015. American Society of Mechanical Engineers (ASME), <http://dx.doi.org/10.1115/OMAE2015-41680>.
- Chai, W., Leira, B.J., 2018. Environmental contours based on inverse SORM. *Mar. Struct.* 60, 34–51. <http://dx.doi.org/10.1016/j.marstruc.2018.03.007>.
- Chen, X., Jiang, Z., Li, Q., Li, Y., Ren, N., 2020. Extended environmental contour methods for long-term extreme response analysis of offshore wind turbines. *J. Offshore Mech. Arct. Eng.* 142, <http://dx.doi.org/10.1115/1.4046772>.
- Coe, R.G., Michelen, C., Eckert-Gallup, A., Sallaberry, C., 2018. Full long-term design response analysis of a wave energy converter. *Renew. Energy* 116, 356–366. <http://dx.doi.org/10.1016/j.renene.2017.09.056>.
- Derbanne, Q., de Hauteclocque, G., 2019. A new approach for environmental contour and multivariate de-clustering. In: Proc. 38th International Conference on Ocean, Offshore and Arctic Engineering, OMAE 2019.
- Dimitrov, N., 2020. Inverse directional simulation: An environmental contour method providing an exact return period. *J. Phys. Conf. Ser.* <http://dx.doi.org/10.1088/1742-6596/1618/6/062048>.
- DNV GL, 2017. Recommended practice DNVGL-RP-C205: Environmental conditions and environmental loads. Technical Report.
- Einmahl, J.H.J., Haan, L.D., Krajina, A., 2013. Estimating extreme bivariate quantile regions. *Extremes* 16, 121–145. <http://dx.doi.org/10.1007/s10687-012-0156-z>.
- Giske, F.I.G., Kvåle, K.A., Leira, B.J., Øiseth, O., 2018. Long-term extreme response analysis of a long-span pontoon bridge. *Mar. Struct.* 58, 154–171. <http://dx.doi.org/10.1016/j.marstruc.2017.11.010>.
- Haghighyeghi, Z.S., Ketabdari, M.J., 2018. A long-term joint probability model for metocean circular and linear characteristics. *Appl. Ocean Res.* 75, 143–152. <http://dx.doi.org/10.1016/j.apor.2018.03.009>.
- Haselsteiner, A.F., Coe, R.G., Manuel, L., Chai, W., Leira, B., Clarindo, G., Guedes Soares, C., Dimitrov, N., Sander, A., Ohlendorf, J.-H., Thoben, K.-D., de Haute, G., Mackay, E., Jonathan, P., Qiao, C., Myers, A., Rode, A., Hildebrandt, A., Schmidt, B., Vanem, E., 2021a. A benchmarking exercise for environmental contours. *Ocean Eng.* 236, <http://dx.doi.org/10.1016/j.oceaneng.2021.109504>.
- Haselsteiner, A.F., Frieling, M., Malte, Mackay, Ed, Sander, Aljoscha, Thoben, Klaus-Dieter, 2021. Long-term response of an offshore turbine: How accurate are contour-based estimates?. *Renewable Energy* 181, 945–965. <http://dx.doi.org/10.1016/j.renene.2021.09.077>.
- Haselsteiner, A.F., Ohlendorf, J.-H., Wosniok, W., Thoben, K.-D., 2017. Deriving environmental contours from highest density regions. *Coast. Eng.* 123, 42–51. <http://dx.doi.org/10.1016/j.coastaleng.2017.03.002>.
- de Hauteclocque, G., Mackay, E., Vanem, E., 2021. Quantitative assessment of environmental contour approaches (preprint from march 2021). <http://dx.doi.org/10.13140/RG.2.2.10068.12161>.
- Haver, S., 1985. Wave climate off northern Norway. *Appl. Ocean Res.* 7, 85–92. [http://dx.doi.org/10.1016/0141-1187\(85\)90038-0](http://dx.doi.org/10.1016/0141-1187(85)90038-0).
- Haver, S., 1987. On the joint distribution of heights and periods of sea waves. *Ocean Eng.* 14, 359–376. [http://dx.doi.org/10.1016/0029-8018\(87\)90050-3](http://dx.doi.org/10.1016/0029-8018(87)90050-3).
- Huseby, A.B., Vanem, E., Natvig, B., 2013. A new approach to environmental contours for ocean engineering applications based on direct Monte Carlo simulations. *Ocean Eng.* 60, 124–135. <http://dx.doi.org/10.1016/j.oceaneng.2012.12.034>.
- Huseby, A.B., Vanem, E., Natvig, B., 2015. Alternative environmental contours for structural reliability analysis. *Struct. Saf.* 54, 32–45. <http://dx.doi.org/10.1016/j.strusafe.2014.12.003>.
- Hyndman, R.J., 1996. Computing and graphing highest density regions. *Amer. Statist.* 50, 120–126. <http://dx.doi.org/10.2307/2684423>.
- International Electrotechnical Commission, 2019. Wind Energy Generation Systems - Part 3-1: Design Requirements for Fixed Offshore Wind Turbines. Technical Report IEC 61400-3-1.
- Jonathan, P., Ewans, K., Flynn, J., 2014. On the estimation of ocean engineering design contours. *J. Offshore Mech. Arct. Eng.* 136, 041101. <http://dx.doi.org/10.1115/1.4027645>.
- Karmakar, D., Bagbanci, H., Guedes Soares, C., 2016. Long-term extreme load prediction of spar and semisubmersible floating wind turbines using the environmental contour method. *J. Offshore Mech. Arct. Eng.* 138, 021601. <http://dx.doi.org/10.1115/1.4032099>.
- Li, Q., Gao, Z., Moan, T., 2016. Modified environmental contour method for predicting long-term extreme responses of bottom-fixed offshore wind turbines. *Mar. Struct.* 48, 15–32. <http://dx.doi.org/10.1016/j.marstruc.2016.03.003>.
- Li, Q., Gao, Z., Moan, T., 2017. Modified environmental contour method to determine the long-term extreme responses of a semi-submersible wind turbine. *Ocean Eng.* 142, 563–576. <http://dx.doi.org/10.1016/j.oceaneng.2017.07.038>.
- Li, L., Yuan, Z.M., Gao, Y., Zhang, X., Tezdogan, T., 2019. Investigation on long-term extreme response of an integrated offshore renewable energy device with a modified environmental contour method. *Renew. Energy* 132, 33–42. <http://dx.doi.org/10.1016/j.renene.2018.07.138>.
- Liu, J., Thomas, E., Goyal, A., Manuel, L., 2019. Design loads for a large wind turbine supported by a semi-submersible floating platform. *Renew. Energy* 138, 923–936. <http://dx.doi.org/10.1016/j.renene.2019.02.011>.
- Mackay, E., Haselsteiner, A.F., 2021. Marginal and total exceedance probabilities of environmental contours. *Mar. Struct.* 75, <http://dx.doi.org/10.1016/j.marstruc.2020.102863>.
- Muliawan, M.J., Gao, Z., Moan, T., 2013. Application of the contour line method for estimating extreme responses in the mooring lines of a two-body floating wave energy converter. *J. Offshore Mech. Arct. Eng.* 135, 031301. <http://dx.doi.org/10.1115/1.4024267>.
- Myers, A.T., Arwade, S.R., Valamanesh, V., Hollowell, S., Carswell, W., 2015. Strength, stiffness, resonance and the design of offshore wind turbine monopiles. *Eng. Struct.* 100, 332–341. <http://dx.doi.org/10.1016/j.engstruct.2015.06.021>.
- Neary, V.S., Ahn, S., Seng, B.E., Allahdadi, M.N., Wang, T., Yang, Z., He, R., 2020. Characterization of extreme wave conditions for wave energy converter design and project risk assessment. *J. Mar. Sci. Eng.* 8, <http://dx.doi.org/10.3390/jmse8040289>.
- Ross, E., Astrup, O.C., Bitner-Gregersen, E., Bunn, N., Feld, G., Gouldby, B., Huseby, A., Liu, Y., Randall, D., Vanem, E., Jonathan, P., 2019. On environmental contours for marine and coastal design. *Ocean Eng.* <http://dx.doi.org/10.1016/j.oceaneng.2019.106194>.
- Sagrilo, L.V.S., Naess, A., Doria, A.S., 2011. On the long-term response of marine structures. *Appl. Ocean Res.* 33, 208–214. <http://dx.doi.org/10.1016/j.apor.2011.02.005>.
- Saranyasoonorn, K., Manuel, L., 2006a. Design loads for wind turbines using the environmental contour method. *J. Sol. Energy Eng.* 128, 554–561. <http://dx.doi.org/10.1115/1.2346700>.
- Saranyasoonorn, K., Manuel, L., 2006b. On assessing the accuracy of offshore wind turbine reliability-based design loads from the environmental contour method. *Int. J. Offshore Polar Eng.* 15, 132–140.
- Serinaldi, F., 2015. Dismissing return periods! *Stoch. Environ. Res. Risk Assess.* 29, 1179–1189. <http://dx.doi.org/10.1007/s00477-014-0916-1>.
- Silva-González, F.L., Vázquez-Hernández, A.O., Sagrilo, L.V.S., Cuamatzi, R., 2015. The effect of some uncertainties associated to the environmental contour lines definition on the extreme response of an FPSO under hurricane conditions. *Appl. Ocean Res.* 53, 190–199. <http://dx.doi.org/10.1016/j.apor.2015.09.005>.
- Vanem, E., Bitner-Gregersen, E.M., 2012. Stochastic modelling of long-term trends in the wave climate and its potential impact on ship structural loads. *Appl. Ocean Res.* 37, 235–248. <http://dx.doi.org/10.1016/j.apor.2012.05.006>.
- Vanem, E., Guo, B., Ross, E., Jonathan, P., 2020. Comparing different contour methods with response-based methods for extreme ship response analysis. *Mar. Struct.* 69, <http://dx.doi.org/10.1016/j.marstruc.2019.102680>.
- Vanem, E., Hafver, A., Nalvarte, G., 2019. Environmental contours for circular-linear variables based on the direct sampling method. *Wind Energy* 1–12. <http://dx.doi.org/10.1002/we.2442>.
- Velarde, J., Vanem, E., Kramhøft, C., Sørensen, J.D., 2019. Probabilistic analysis of offshore wind turbines under extreme resonant response: Application of environmental contour method. *Appl. Ocean Res.* 93, <http://dx.doi.org/10.1016/j.apor.2019.101947>, 101947.
- Wang, S., Wang, X., Woo, W.L., 2018. A comparison of response-based analysis and environmental contour methods for FPSO green water assessment. In: Proc. 37th International Conference on Ocean, Offshore and Arctic Engineering, OMAE 2018. American Society of Mechanical Engineers (ASME), Madrid, Spain, <http://dx.doi.org/10.1115/OMAE2018-77841>.
- Winterstein, S.R., Jha, A.K., Kumar, S., 1999. Reliability of floating structures: extreme response and load factor design. *J. Waterw. Port Coast. Ocean Eng.* 125, 163–169. [http://dx.doi.org/10.1061/\(ASCE\)0733-950X\(1999\)125:4\(163\)](http://dx.doi.org/10.1061/(ASCE)0733-950X(1999)125:4(163)).
- Winterstein, S.R., Ude, T.C., Cornell, C.A., Bjerager, P., Haver, S., 1993. Environmental parameters for extreme response: Inverse FORM with omission factors. In: Proc. 6th International Conference on Structural Safety and Reliability, ICOSSAR 93. Innsbruck, Austria.
- Xu, Y., Øiseth, O., Moan, T., Naess, A., 2018. Prediction of long-term extreme load effects due to wave and wind actions for cable-supported bridges with floating pylons. *Eng. Struct.* 172, 321–333. <http://dx.doi.org/10.1016/j.engstruct.2018.06.023>.